

Consistent Large-Signal Modeling of SiGe HBT Devices

Tom K. Johansen, Jens Vidkjær, Viktor Krozer

Technical University of Denmark, Oersted-DTU, Department of Electromagnetic Systems,
Oersteds Plads 348, 2800 Kgs. Lyngby, Denmark, +45-45253770, tkj@oersted.dtu.dk

Abstract—In this paper the applicability of the VBIC95 model for consistent modeling of SiGe HBT devices is investigated. A parameter extraction method is described, including quasi-saturation, substrate parasitics, self-heating and weak avalanche multiplication. Consistency between large-signal and bias-dependent small-signal modeling is assured by extraction several VBIC95 model parameters from a dedicated small-signal model. The VBIC95 model is experimentally verified against DC and RF measurements on a $8 \times 0.35 \mu\text{m}^2$ area SiGe HBT device.

I. INTRODUCTION

SiGe HBT technology has gained increasing importance in wireless, mixed-signal, and high-speed applications. Among the benefits are low-cost, high-speed devices, good noise performance and compatibility with CMOS technology. In order to cover a broad range of different circuit applications consistent large-signal and bias-dependent small-signal modeling of the SiGe HBT devices becomes an important issue.

In the design of integrated circuits compact models such as SGP, HICUM, MEXTRAM or VBIC95 are indispensable [1]. Though developed for homojunction devices the VBIC95 model includes several features important to accurately model modern SiGe HBT devices. These include modeling of fixed oxide capacitances, quasi-saturation, substrate parasitics, self-heating and weak avalanche multiplication [2]. Modeling issues specific to SiGe HBT devices are the different temperature dependence due to different effective bandgaps in the base and emitter regions, high injection effects at the base-collector heterojunction leading to a conduction band barrier, and nonnegligible base current component due to neutral-base recombination [3]. Temperature dependence for SiGe HBT devices with both box Ge and graded Ge profiles can be accurately modeled with the VBIC95 model [4], [5]. The heterojunction barrier effect and neutral-base recombination is usually avoided by proper SiGe HBT profile optimization [6]. More serious concerns for SiGe HBT modeling with VBIC95 are the bias dependent modeling of intrinsic base resistance, base-collector capacitance, excess phase delay and the quasi-saturation modeling.

In this work a VBIC95 model parameter extraction methodology leading to consistent large-signal modeling for SiGe HBT devices is presented. A dedicated small-signal model for the SiGe HBT device is used to extract several VBIC95 parameters of interest for the high frequency modeling. The variation of the elements of the small-signal model over bias provide a discussion of the VBIC95 model accuracy. The VBIC95 model is experimentally verified in the range from DC to 26.5 GHz on a $8 \times 0.35 \mu\text{m}^2$ area SiGe HBT device.

II. DC PARAMETER EXTRACTION

The parameter extraction in this section is concerned with the static VBIC95 model. Because the main current are formulated in terms of the depletion charges this includes the extraction of the parameters for the junction capacitances. The parameter extraction is based on measurements on a $8 \times 0.35 \mu\text{m}^2$ area SiGe HBT device.

A. Junction Capacitances

The total input and feedback capacitances are extracted from S-parameters using cut-off mode measurement over reverse and slightly forward biased junctions [7]. In modern double-poly SiGe HBT devices the measured capacitance may include significant contribution from fixed oxide capacitance. In order to accurately determine the junction capacitance parameters the fixed oxide capacitances have to be taken into account. In order to assess the importance of the fixed oxide capacitance C_{beo} on the base-emitter junction capacitance parameters the quantity $C_{meas} - C_{beo}$ is plotted on a double-logarithmic graph versus $1 - V_{be}/P_e$ where V_{be} and P_e are the junction potential and built-in potential, respectively. As shown in Fig. 1 a straight line is only achievable when the fixed oxide capacitance is taken into account. Once the junction capacitance parameters M_e , P_e , M_c , and P_c are known the forward and reverse Early voltage parameters V_{ef} and V_{er} are extracted using the standard method [8].

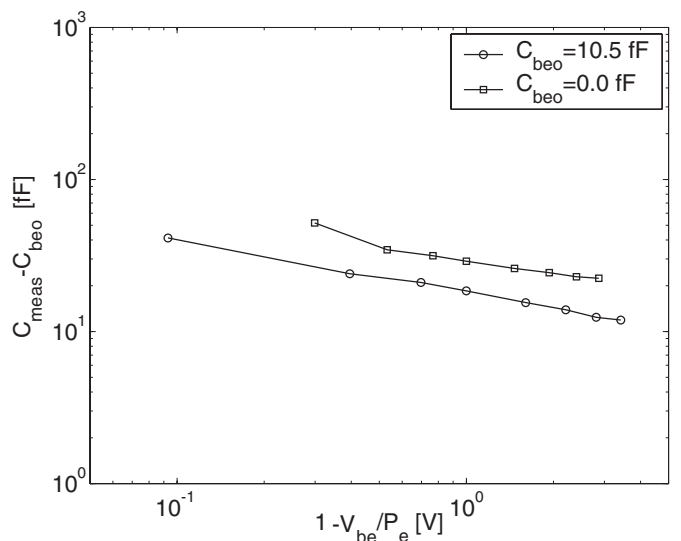


Fig. 1. Importance of fixed oxide capacitance on base-emitter junction parameters.

B. Gummel Measurements

The forward transport current parameters I_s and N_f and base-emitter current parameters I_{be_i} , N_{ei} , I_{be_n} and N_{en} are extracted from forward Gummel measurement in the range from 0.4-0.8V. The substrate transistor transport current parameters I_{sp} and N_{fp} and parasitic base-collector current parameters I_{bcip} , N_{cip} , I_{bcnp} and N_{cnp} are extracted from the reverse gummel plot of the parasitic substrate transistor. The extraction of the base-collector current parameters I_{bc_i} , N_{ni} , I_{bc_n} and N_{cn} are performed with saturated substrate transistor. The parameters for substrate transistor transport including the knee-current parameter I_{kp} are refined together with the base-collector current parameters by optimization to fit the measured reverse beta characteristic in the range from 0.4-0.8V. The fixed access resistance parameters R_{bx} , R_e , and R_{cx} are extracted from S-parameters using saturation mode measurements with forced base currents [7].

C. I_c - V_{ce} Characteristic

From the forward output characteristic in the linear region where quasi-saturation, and weak avalanche multiplication are negligible the forward knee current I_{kf} is extracted. To take self-heating into account the thermal resistance R_{th} is extracted from the decrease of the base-emitter voltage in the output characteristic at constant base current. The activation energy parameter E_a for the transfer current depends on the bandgap narrowing due to doping and Ge-grading across the base region. Neglecting the doping induced bandgap narrowing the effective bandgap can be estimated as

$$E_a = E_{g,Si} - \Delta E_{g,SiGe} \quad (1)$$

where $E_{g,Si}$ is the bandgap of Si and $\Delta E_{g,SiGe}$ is the effective bandgap narrowing due to the Ge-grading which depends on the peak Ge content in the base. If ΔE_g is the bandgap narrowing at the base-collector junction the average over the base region gives [3]

$$\Delta E_{g,SiGe} = -k_B T \ln \left(\frac{k_B T}{\Delta E_g} \left(1 - \exp \left(\frac{-\Delta E_g}{k_B T} \right) \right) \right) \quad (2)$$

where T is the absolute temperature and k_B is boltzmann constant. Assuming a bandgap narrowing of 7.5 meV per percent Ge-content [6], a typical linear graded profile with a peak Ge value of 15 percent and a default value of $E_{g,Si} = 1.12eV$ the estimate for the activation energy parameter becomes $E_a = 1.082eV$.

It is well-known that the extraction of the epi-layer parameters R_{ci} , γ , V_o and H_{rcf} from the quasi-saturation region of the forward output characteristic will affect the fall-off of reverse beta at high currents [9]. Therefore a iteration scheme should be followed in the extraction of the epi-layer parameters. First the reverse knee current parameter $I_{kr} = I_{kf}$ is used in the extraction. Next the reverse knee current parameter is refined by optimization to fit reverse beta. The epi-layer parameters are then re-extracted with this knee current and good agreement in both forward output and reverse beta characteristic is obtained. The modeling of the forward output characteristic is completed with the extraction of the weak avalanche multiplication parameters A_{vc1} and A_{vc2} .

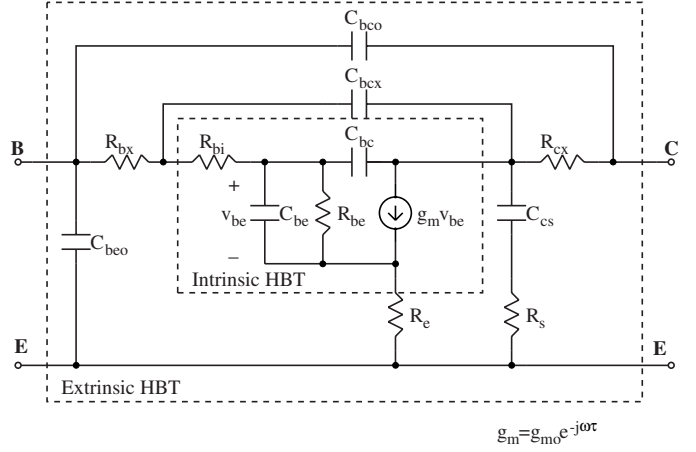


Fig. 2. Dedicated small-signal equivalent circuit model for SiGe HBT device in forward active region.

III. AC PARAMETERS EXTRACTION

The extraction of the VBIC95 model parameters of interest for the ac-modeling includes the intrinsic base resistance R_{bi} , base-collector depletion capacitance partitioning between C_{jc} and C_{jep} , forward transit time T_f , excess phase delay T_d , and the epi-layer charge Q_{co} important in quasi-saturation. Notice that the SGP transit time parameters X_{tf} , I_{tf} , V_{tf} and T_r should be omitted when the epi-layer parameters is included [9]. Several of these parameters can be extracted from the bias dependence of the intrinsic elements for the dedicated small-signal equivalent circuit model shown in Fig. 2. All elements for this equivalent circuit model is found by direct parameter extraction using the multi-step de-embedding approach reported in [7]. Table I gives a summery of the extracted elements for the small-signal equivalent circuit model at the bias point $V_{ce} = 1.5V$ $I_c = 4.3mA$ corresponding to peak f_T .

In VBIC95 the intrinsic base resistance is modeled as R_{bi}/q_b , where q_b is the normalized base charge. As the collector current I_c goes toward zero, the normalized base charge becomes $q_b \approx 1$. The extraction of the VBIC95 intrinsic base resistance parameter R_{bi} is then achieved by extrapolating extracted values of intrinsic base resistance versus collector current onto the ordinate axis, as shown in Fig. 3. This figure also shows the intrinsic base resistance as calculated by the VBIC95 model. The conductivity modulation model in VBIC95 is not able to predict accurately the current dependence observed for the intrinsic base resistance at low current levels.

The reduction in the base-collector depletion capacitance

Parameter	Value	Parameter	Value
R_{bx} [Ω]	14.0	C_{be} [fF]	326.0
R_e [Ω]	5.5	R_{be} [Ω]	966.7
R_{cx} [Ω]	6.0	g_{m0} [mS]	135.6
C_{beo} [fF]	10.5	τ [ps]	0.17
C_{bco} [fF]	≈ 0	C_{bcx} [fF]	7.5
R_{bi} [Ω]	29.5	C_{cs} [fF]	15.5
C_{bc} [fF]	5.9	R_s [Ω]	1066

TABLE I
EXTRACTED ELEMENTS FOR SMALL-SIGNAL MODEL
($V_{ce} = 1.5V$ $I_c = 4.3mA$).

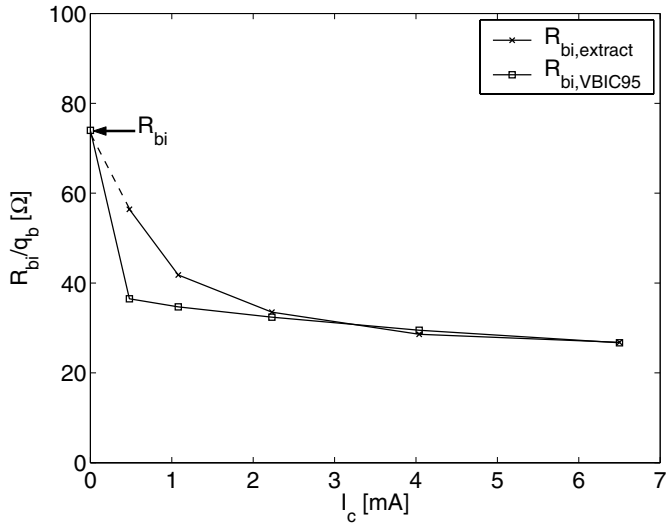


Fig. 3. Extracted intrinsic base resistances compared with the conductivity modulation model in VBIC95 ($V_{ce} = 1.5V$). The VBIC95 model base resistance parameter is $R_{bi} = 74\Omega$.

with current due to mobile charge modulation effects is not modeled in VBIC95. From the extracted values of intrinsic base-collector capacitance versus collector current as shown in Fig. 4 an slight increase rather than a decrease is observed. This implies that voltage drop across the undepleted part of the epilayer dominates over charge modulation effects [3]. The VBIC95 model accurately models this effect with inclusion of the epi-layer parameters. The partitioning of the VBIC95 model parameters C_{jc} and C_{jep} follows the ratio between the extracted intrinsic and extrinsic base-collector capacitances at low currents.

In order to extract the forward transit time parameter T_f , values of base-emitter capacitance C_{be} and transconductance g_{mo} are used to calculate the forward transit time as

$$\tau_f = \frac{C_{be} - C_{be,co}}{g_{mo}} \quad (3)$$

where $C_{be,co}$ is the extracted base-emitter depletion capaci-

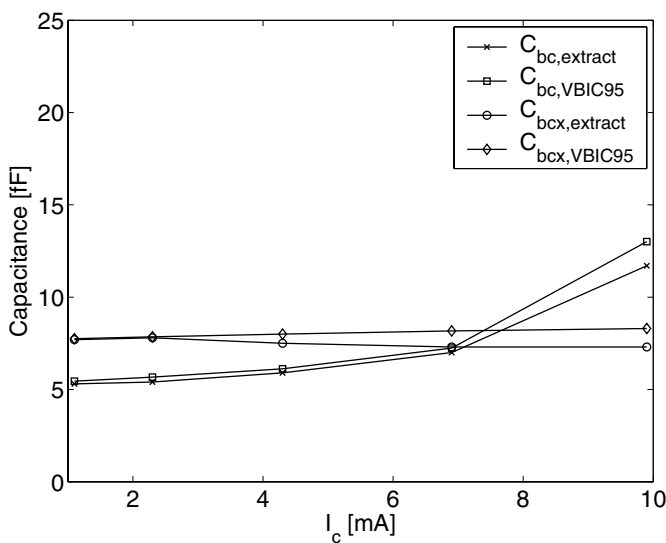


Fig. 4. Bias dependence of extracted intrinsic and extrinsic base-collector capacitances ($V_{ce} = 1.5V$).

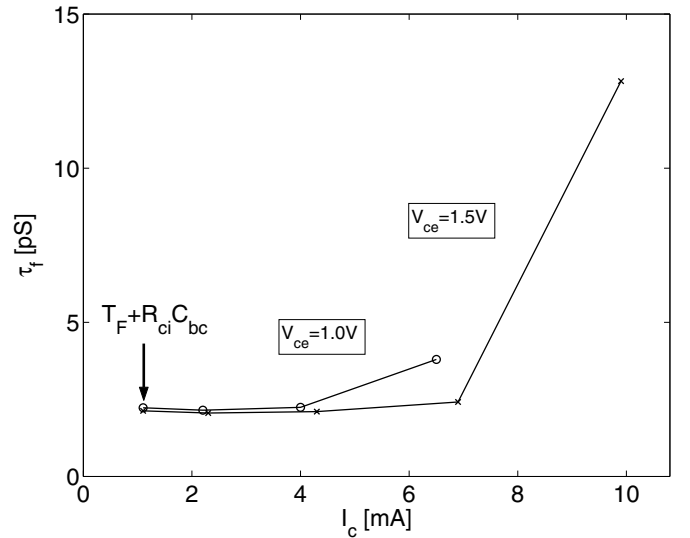


Fig. 5. Extraction of forward transit time parameter T_f at.

tance for a slightly forward biased junction. In Fig. 5 calculated values of τ_f are plotted versus I_c for two different collector-emitter voltages. Due to the epi-layer resistance in the VBIC95 model an additional contribution ($R_{ci}C_{bc}$) to the transit time is present. The forward transit time parameter T_f needs to be corrected for this contribution to accurately contribute to the cut-off frequency. The epi-layer charge Q_{co} is extracted from the measured cut-off frequency f_T characteristic in the high current region.

The inclusion of non-quasi static effects in the VBIC95 model is done with a bias independent excess phase delay parameter T_d . However as reported previously [7], the excess phase delay in SiGe HBT devices will increase once base widening effects becomes noticeable. Therefore the extracted value of τ at peak f_t , is used for T_d . This gives a good compromise in the description of non-quasi static effects between the low- and high-current regimes.

IV. EXPERIMENTAL VERIFICATION

The model results in this section are performed using the built-in VBIC95 model in Agilent ADS. The measured and modeled forward Gummel characteristic is compared in Fig. 6. The model predicts the measured characteristic accurately even in the high current region. The observed kink in the base current indicates the onset of quasi-saturation. In Fig. 7 the measured I_c - V_{ce} characteristic is compared with the model result. Good agreement is observed over the four different regions: saturation, quasi-saturation, linear, and breakdown.

Fig. 8 compare the measured and modeled bias dependence for the cut-off frequency f_T . An excellent agreement is obtained proving the consistency in large-signal and small-signal modeling of quasi-saturation in the VBIC95 model.

Fig. 9 compare the measured and modeled S-parameters in the frequency range from 45 MHz-26.5 GHz after a three step de-embedding method [10] was employed to remove the influence from pad and interconnect line parasitics. The bias point is $V_{ce} = 1.5V$, $I_c = 4.3mA$ corresponding to peak f_T for the device. Both the dedicated small-signal model and the VBIC95 model are observed to be in good agreement with measurements.

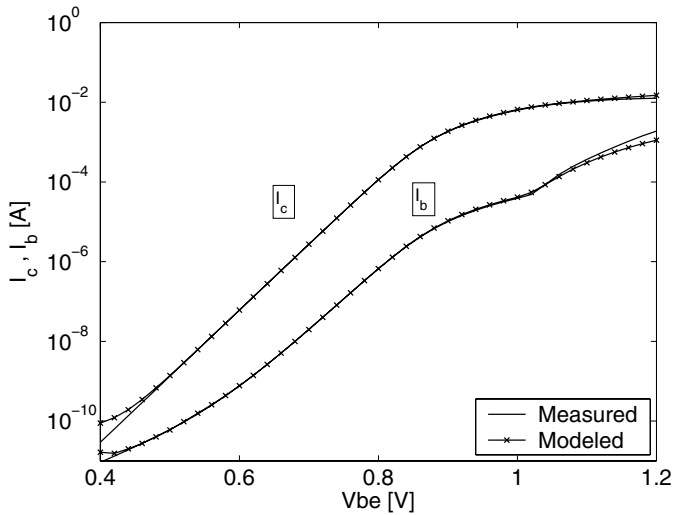


Fig. 6. Measured and modeled forward Gummel characteristic measured at $V_{cb} = 0.0V$.

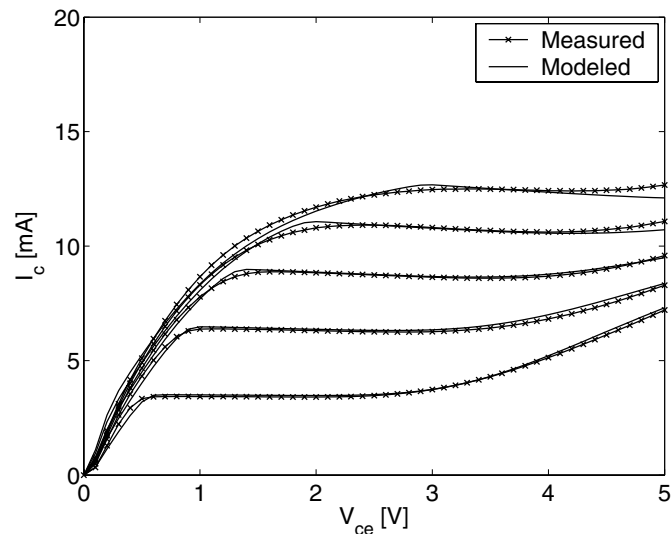


Fig. 7. Measured and modeled I_c - V_{ce} characteristic for I_b swept from 20 – 100 μA .

V. CONCLUSIONS

The applicability of the VBIC95 model for consistent large-signal modeling of SiGe HBT devices has been investigated. A parameter extraction method is described leading to good agreement between large-signal and bias-dependent small-signal modeling. The bias dependent elements, which are important for the high frequency modeling of SiGe HBT devices with VBIC95, have been compared with elements extracted from a dedicated small-signal model. The experimental results demonstrate the consistency between large-signal and bias-dependent small-signal modeling for SiGe HBT devices using VBIC95.

ACKNOWLEDGEMENT

The authors wish to acknowledge Mattias Ferndahl, Chalmers Institute of Technology, Goteborg, Sweden for helping with the S-parameter measurements.

REFERENCES

[1] H. C. de Graaff, "State-of-the-Art in Compact Modelling with Emphasis on Bipolar RF Circuit Design," in *Proc. ESSDERC*, 1997.

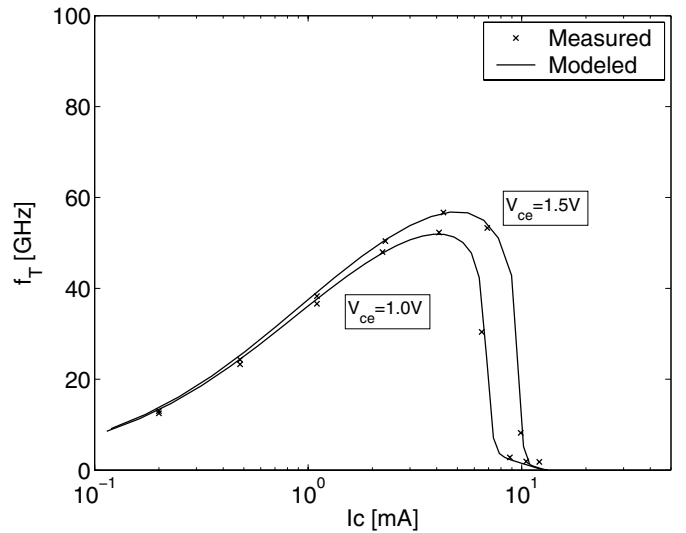


Fig. 8. Measured (x) and modeled (-) bias dependence for the cut-off frequency f_T .

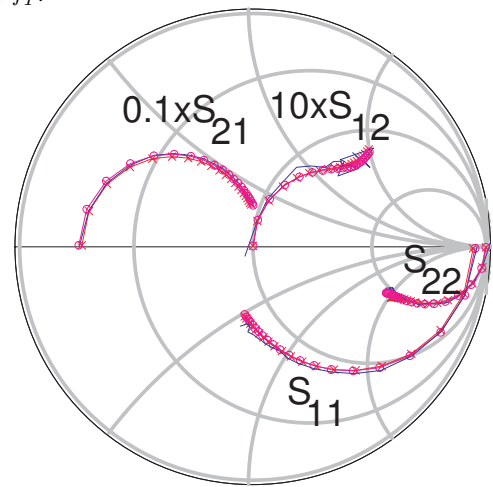


Fig. 9. Comparing measured (-) S-parameters with dedicated small-signal model (-x-) and VBIC95 model (-o-) in the forward active region (45MHz – 26.5GHz, $V_{ce} = 1.5V$, $I_c = 4.3mA$).

- [2] C. C. M. et al., "VBIC95, The Vertical Bipolar Inter-Company Model," *IEEE Journal of Solid-State Circuits*, vol. 31, no. 10, pp. 1476–1483, Oct. 1996.
- [3] M. Reisch, *High-Frequency Bipolar Transistors*. Springer, 2003.
- [4] F. X. Sinnesbichler and G. R. Olbrich, "Electro-Thermal Large-Signal Modeling of SiGe HBTs," in *Proc. EuMW2004*, Oct 1999, pp. 125–128.
- [5] M. R. Murty, "Implementation of a Scalable and Statistical VBIC Model for Large-Signal and Intermodulation Distortion Analysis of SiGe HBTs," in *IEEE MTT-S Digest*, 2002, pp. 2165–2168.
- [6] J. D. Cressler and G. Niu, *Silicon-Germanium Heterojunction Bipolar Transistors*. Artech House, 2003.
- [7] T. K. Johansen, J. Vidkjær, and V. Krozer, "Substrate Effects in SiGe HBT Modeling," in *Proc. GAAS2003*, Oct 2003, pp. 445–448.
- [8] C. C. McAndrew and L. W. Nagel, "SPICE Early Modeling," in *IEEE BCTM*, 1994, pp. 144–147.
- [9] W. J. Kloosterman, "Comparison of Mextram and the VBIC95 bipolar transistor model," Philips Electronics N.V. Nat. Lab. Unclassified Report 034/96, Tech. Rep., 1996.
- [10] H. Cho and D. Burk, "A Three-Step Method for the De-Embedding of High-Frequency S-Parameter Measurements," *IEEE Transaction on Electron Devices*, vol. 38, no. 6, pp. 1371–1375, Jun. 1991.